Available online at www.sciencedirect.com

ScienceDirect

Procedia Structural Integrity 62 (2024) 400–407

Structural Integrity Procedia

www.elsevier.com/locate/procedia

II Fabre Conference – Existing bridges, viaducts and tunnels: research, innovation and applications (FABRE24)

An experimental campaign for assessing the role of tensioned tendons on the shear capacity of half-joints

Riccardo Martini[a,*], Lorenzo Amico[a], Vanni Nicoletti[a], Sandro Carbonari[a], Laura Ragni[a], Fabrizio Gara[a]

[a] *Dept. of Construction, Civil Engineering and Architecture (DICEA), Università Politecnica delle Marche, Ancona, Italy*

Abstract

An important percentage of bridges and viaducts constituting the Italian road infrastructures dates back to the years 50s and 60s and is characterized by prestressed r.c. decks adopting half-joints for obtaining statically determinate schemes. In existing bridges, half-joints are often subjected to degradation phenomena, mostly promoted by water percolation and stagnation, which led to classify the bridge in a high attention class, according to the Italian Guidelines for Risk Classification and Management, Safety Assessment and Monitoring of Existing Bridges. Furthermore, half-joints are difficult to inspect and to maintain. The current safety assessment procedures at ultimate limit state are based on simplified Strut&Tie models that usually neglect the contribution of prestressing tendons anchored in the half-joints on the resisting mechanisms and the ultimate capacity. This work presents the design of an experimental campaign for investigating the shear behaviour and the ultimate capacity of half-joints in which inclined prestressed tendons are anchored. In detail, six laboratory scaled post-tensioned beams are built with half-joints in correspondence of the support regions, dimensioned on the basis of a real bridge girder and numerical 3D finite element nonlinear analyses. The main research goal is to evaluate the influence of tendons on the half-joints capacity by comparing results with those obtained from specimens with non-tensioned tendons and without tendons. Three levels of pre-tensions in specimens characterized by the same reinforcements are considered. In addition, for one level of pre-tension, the effects of different half-joints detailing are investigated. Finally, the role of degradation due to ageing is also addressed by inducing corrosion in one specimen through a galvanic method.

Keywords: Ageing effects; experimental tests; half-joints; prestressed bridge girders; reinforcement corrosion; shear failure

* Corresponding author. Tel.: +0-000-000-0000 ; fax: +0-000-000-0000 .
E-mail address: r.martini@pm.univpm.it

10.1016/j.prostr.2024.09.058

1. Introduction

Most of the existing bridges belonging to the Italy's road infrastructure date back to the 1950s and 1960s, when the concrete prestressing techniques were developed and largely employed in bridge engineering. The use of precast prestressed beams made it possible to speed up the construction phases and to improve the overall performance of concrete beams, with an average increase of the span length. Commonly, statically determinate structural schemes were used, such as simply supported beams or Gerber beams, which usually require the use of particular construction details, namely the half-joints at the beam ends. The use of half-joints, which were mandatory in case of Gerber beams, were often used also in case of simply supported deck. In existing bridges, half-joints are today often subjected to material degradation phenomena due to ageing, mostly promoted by percolation and water stagnation favoured by the particular geometry of the element; thus, these elements are often characterized by cracking phenomena, with patterns consistent with their collapse mechanisms. According to the Italian Guidelines for Risk Classification and Management, Safety Assessment and Monitoring of Existing Bridges [Linee Guida Ponti (2020)], the half-joints constitute critical elements for the stability of the structure because they are characterized by brittle failure mechanisms that may lead to the sudden collapse of the structure. Consequently, in addition to standard visual inspections, special inspections are mandatory to investigate the state of preservation of critical elements, such as half-joints or prestressing cables, whose degradation may be responsible of similar brittle failure mechanisms.

Half-joints, especially those hosting anchorages of prestressed cables, turn out to be construction details sensitive to damage, difficult to inspect and to maintain. Therefore, the presence of degradation phenomena or defects in half-joints leads to classify the bridge in a high attention class, for which an accurate safety assessment procedure must be carried out. The national or international codes provide standard procedures to assess half-joints based on simplified Strut&Tie models, which are generally very conservative, or very difficult to conceive if the strength contributions offered by prestressing cables and residual tensioning levels have to be considered. Many studies are reported in the literature investigating the capacity of half-joints to shear stresses and many simplified Strut&Tie models are proposed and experimentally validated [Mattock and Chan (1979), Schlaich at al. (1987) and Mader (1990)]. The geometry of the element, the amount of reinforcement, the reinforcement configurations, and the possible presence of damage are among the most frequently investigated issues [Lin et al. (2003) and Desnerck et al. (2016 and 2017)]. However, only few works concern the capacity of pre-stressed half-joints and the evaluation of the strength contribution offered by the residual tensioning stress of strands anchored in the element [Moreno-Martínez and Meli (2014)].

This paper presents the design of an experimental campaign aimed to study the shear behaviour and ultimate capacity of half-joints in which inclined pre-stressed tendons are anchored. The campaign involves tests on six laboratory pre-tensioned beams with half-joints at the support regions, scaled on the basis of a real bridge girder. For the proper design of the test and the beam reinforcements beyond the disturbed region of the half-joint, numerical analyses are performed with both simplified Strut&Tie models, as reported on international standards, and refined 3D nonlinear finite element models. The main objective of the research is to evaluate the influence of post-tensioned tendons on the capacity of the half-joint by comparing results with those obtained from specimens with different levels of residual prestress. For this reason, three different levels of pre-tensioning were considered on specimens characterized by the same reinforcements, including the case with no-tensioning and the complete absence of strands. In addition, for a selected level of pre-tensioning, effects due to a 50% reduction in shear reinforcement on the ultimate shear capacity are investigated. Finally, the role of steel degradation is also addressed by inducing corrosion on the main reinforcements through a galvanic method for a specimen at a fixed stress level.

2. Laboratory half-joint beam design and testing

The design of the laboratory beams with half-joints is based on prestressed beams of an existing bridge built in the 1980s. The bridge is characterized by 8 spans of 35 meters long simply supported beams, for a total length of 280 m. The deck consists of 1.8 m high and 0.65 m wide I-shape cross-section beams characterized by half-joint supports at both ends. The latter are constituted by 0.85 m high and 0.97 m depth nibs, so that the geometric ratio between the height and the depth of the nib is equal to 1.14 (see Fig. 1a). The post-tensioning system involves five prestressing cables made of wire strands constituted by 32 wires with diameter of 7 mm. The path of cables along the beam is curvilinear, which is typical for simply supported beams. Four prestressing cables are anchored on the half-joint of

the beam, while the remaining cable is anchored on the top flange of the beam (Fig. 1b) and it is probably tensioned after the slab cast. The half-joints have a reinforcement layout consisting of both vertical and horizontal reinforcements constituted by 4ϕ20 and 4ϕ16, respectively, positioned in such a way as to stitch the nib with the full-depth cross-section of the beam, and by 4ϕ20 diagonal reinforcements inclined of 45° (Fig. 1c). Within the disturbed region of the half-joint, which extends approximately for a length equal to one times the full-depth cross-section, a refinement of the beam stirrups spacing is also provided.

The laboratory specimens are designed by adopting a scale factor of 3, and a geometric ratio of the nib height to the nib depth equal to 1. The full-depth cross-section of the beam has dimensions of 0.22 x 0.6 m, while at the support regions the cross-section has dimensions 0.22 x 0.3 m. The specimens have a total length of 4.1 m, in order to mitigate the shear forces along the beam for the collapse force, and foresees half-joints on both ends to double the number of elements to be tested. A C40/50 concrete class with a S5 workability class is selected during the design, while the actual elastic modulus and the ultimate compressive strength of the material will be obtained through experimental tests on cylindrical samples to be taken during the beam casting.

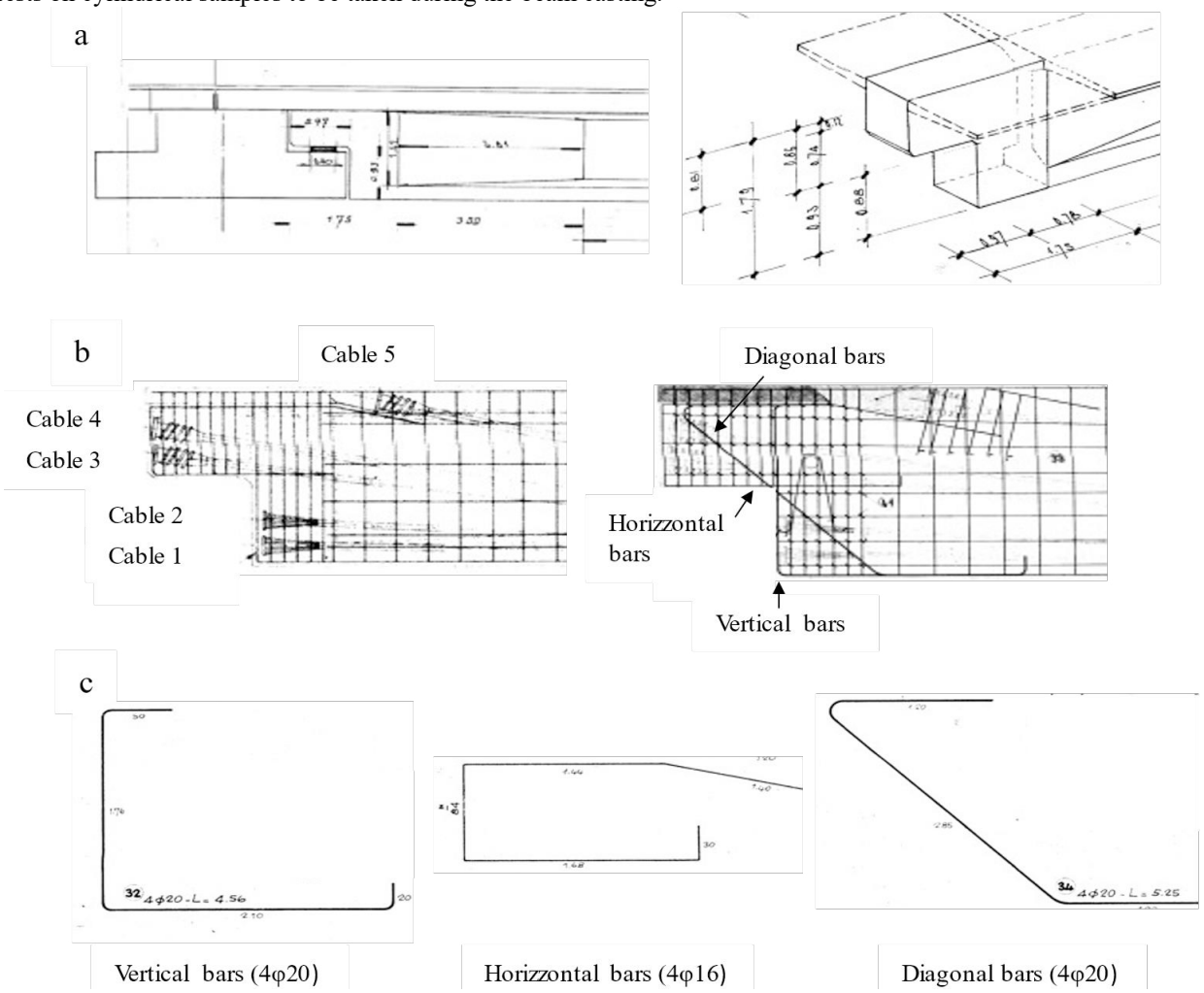

Fig. 1. (a) Geometry of the existing bridge girder; (b) post-tensioning system and reinforcement layout; (c) half-joint reinforcements.

A B450C steel grade is adopted for steel, while Dywidag bars are used for the prestressing system. The main reinforcement configuration of the specimen half-joints, Layout A (Fig. 2a), is inspired by the existing bridge girder reinforcement configuration, taking into account the previously mentioned scale factor. In detail, the same amount of

reinforcement was adopted for both vertical, horizontal, and diagonal bars (2ϕ8+2ϕ6). The four prestressing cables anchored into the half-joint (Fig. 1b) are reproduced by inserting two Dywidag WR18 Threadbars. The anchored top bar is cold bent with a radius of curvature equal to 8 m, in order to obtain the 8 degrees inclination of the cables, as in the existing bridge beam. Both the prestressing bars are anchored by means of an external square anchor plate. Finally, four-legged stirrups with a 10 cm spacing on the nib and two-legged stirrups with a 13 cm spacing on the full-depth cross-section are adopted. Layout B is obtained by modifying Layout A to achieve a 50% reduction of the stirrups on the half-joint (Fig. 2b), while Layout C (Fig. 2c) is similar to Layout A but it lacks of prestressing bars. Layouts B and C are adopted to study the influence of the shear reinforcement in the nib, while Layout C is intended to provide the benchmark data for most of the comparisons. To investigate the influence of the prestressing level and the presence of corrosion on the main reinforcement bars of the half-joint on the ultimate capacity, four specimens are made with reinforcement Layout A; these are distinguished by three different levels of prestressing: 0 MPa (i.e. no prestress), 640 MPa, and 760 MPa. The specimen subjected to induced corrosion is assigned the maximum level of prestressing. All the specimens are equipped with 3ϕ18 at the bottom of the cross-section in order to avoid a flexural failure in the inner sections of the beam during the tests; these reinforcements are not obtained from a consistent scaling of the reference bridge beam and are anchored at the beam end through hooks in order to avoid any interaction with the half-joint resisting mechanism. Preliminary finite element numerical investigations confirmed that they have no relevance on the half-joint capacity. Construction details and prestressing levels of specimens are summarized in Table 1, where a label is also assigned to each specimen.

The unsymmetrical three-point bending test is used with a statically determinate support system (roller and pinned steel supports); the total distance between the axes of the two supports is 3580 mm. The quasi-static load is applied with an hydraulic jack placed 800 mm away from the half-joint support (Fig. 3).

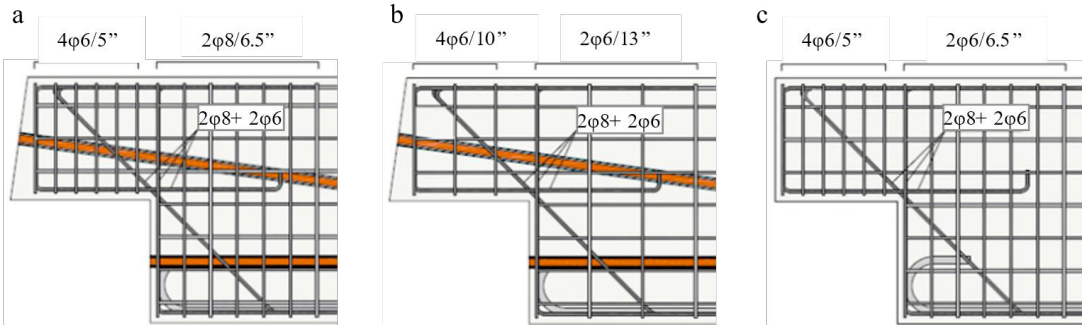

Fig. 2. (a) Reinforcement layout A; (b) Reinforcement layout B; (c) Reinforcement layout C.

Table 1. Reinforcement details and prestressing level of the specimens.

Specimen Name	Layout	Prestressing	Vertical rebars	Horizontal rebars	Diagonal rebars	Nib stirrups	Full-depth stirrups
[-]	[-]	[MPa]	[mm^2]	[mm^2]	[mm^2]	[-]	[-]
RL-A1	A	760	157.08	157.08	157.08	4φ8/5”	4φ8/6.5”
RL-A2	A	640	157.08	157.08	157.08	4φ8/5”	4φ8/6.5”
RL-A3	A	0	157.08	157.08	157.08	4φ8/5”	4φ8/6.5”
RL-A1D	A	760	125.66	125.66	125.66	4φ8/5”	4φ8/6.5”
RL-B1	B	760	157.08	157.08	157.08	4φ8/10”	4φ8/13”
RL-C	C	-	157.08	157.08	157.08	4φ8/5”	4φ8/6.5”

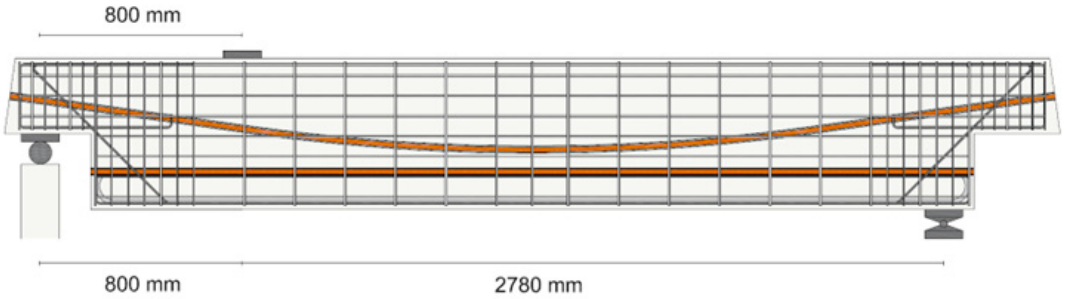

Fig. 3. Test configuration layout.

The position of the load is suitably studied, through preliminary numerical analyses in order to exclude significant arch effect in the load transfer mechanism as well as to limit a high bending moment to be entrusted with longitudinal rebars in order to avoid that the ductile flexural mechanism anticipates the fragile shear one. Also, the beam length is defined to limit the shear reinforcements outside the half-joint sections.

3. Numerical analysis

The ultimate capacity of the specimens was evaluated numerically by adopting Strut&Tie models, according to the FABRE technical document for the safety assessment of half-joint beams [FABRE (2022)], and by using nonlinear finite element models. The objective of the numerical analyses is twofold: (*i*) to estimate the ultimate capacity of the elements for a proper sizing of the bending and shear reinforcements of the beams outside the disturbed region, with the aim to prevent the bending failure, and (*ii*) to define the test instrumentation typology and layout, starting from the analysis of the numerical predictions.

3.1. Strut-and-tie models

The ultimate capacity of prestressed specimens RL-A1, RL-A2, RL-A1D, and RL-B1 is evaluated by adopting a Strut&Tie model that combines the two main resistant mechanisms offered by vertical and horizontal reinforcements, and diagonal reinforcements. The model is suitably modified to include the contribution of prestressing forces P_1 and P_2 (Fig. 4a,b) by introducing the two additional nodes 10 and 11 at the anchor plates of the prestressing rebars. The resulting Strut&Tie mechanism is statically indeterminate; however, by applying the plastic truss method, it can be divided into two statically determined systems, corresponding to two stages of the resisting mechanisms. The first stage (Fig. 4a) foresees the achievement of yielding of both vertical and diagonal ties ($T_{3\text{-}6}$ and $T_{2'\text{-}7}$); at this point, due to the contribution of prestressing force P_1, tendon $T_{1\text{-}5}$ is compressed, and strut $C_{1\text{-}2'}$ has reached its limiting compressive force imposed by the equilibrium of node 2'. The second stage (Fig.4b) foresees the formation of a new load path $C_{1\text{-}4}$ (in red), which allows R_C and the tensile stress on strut $C_{1\text{-}5}$ to increase progressively. For the equilibrium conditions of node 4, tendon $T_{4\text{-}5}$ must also be formed. The ultimate capacity of the half-joint is calculated at the yielding of all the main reinforcements, i.e., once the horizontal reinforcement has reached yielding in the second phase of the resisting mechanism. The ultimate capacity of the specimen without prestressing RL-C is calculated in a more conventional way by combining the two main resistant mechanisms offered by the vertical and horizontal reinforcements, and the diagonal reinforcements.

The first resisting mechanism (Fig. 5a) is statically determined and can be solved by imposing equilibrium of the internal nodes and global rotational equilibrium around node 7. The ultimate capacity is limited by the resistance of ties $T_{1\text{-}5}$ and $T_{3\text{-}6}$; the former governing the capacity for specimen RL-C. The second resistant mechanism (Fig. 5b) is based on the contribution of the diagonal reinforcements; the Strut&Tie model is statically determined and can be solved by imposing the translational equilibrium of the internal nodes. The ultimate capacity of the mechanism is limited by the yielding of tie $T_{2\text{-}7}$. The expected ultimate capacity of all the half-joints are summarized in Table 2.

Table 2. Ultimate capacity of the half-joints with strut-and-tie models.

Specimen Name [-]	Ultimate capacity [kN]	Specimen Name [-]	Ultimate capacity [kN]	Specimen Name [-]	Ultimate capacity [kN]
RL-A1	211.19	RL-A3	120.22	RL-B1	185.17
RL-A2	199.00	RL-A1D	211.19	RL-C	120.22

3.2. Refined 3D models

The ultimate capacity of the specimens are also calculated by performing non-linear analyses on refined solid models developed in ANSYS environment. The nonlinear Menetrey-William geomechanics model, that includes combined hardening and softening functions for compression stresses and a softening curve for tensile stresses, is adopted for concrete (Fig. 6a). Two bilinear constitutive laws with isotropic hardening are defined for the reinforcements and for the high-tensile rebars (Dywidag). The 3D hexahedral CPT215 solid element available in ANSYS is used for concrete (Fig. 6b) while the embedded reinforcements are modelled with the REINF264 element (red lines in Fig. 7a), and rebars of the post-tensioning system are schematized with the BEAM188 element, based on the classic Timoshenko beam theory (blue lines in Fig. 7a). Interactions between finite elements are managed using the multi-points constraint formulation (MPC). The mesh is obtained by imposing a sizing of 40 mm in the half-joint region and 50 mm for the remaining part of the beam using the hex dominant method. After the meshing, a total of 16541 nodes and 13342 elements are obtained (Fig. 7b). The modelling strategy is validated by reproducing results of the three-points bending test for NS-REF half-joint specimen of the experimental campaign conducted by the Desnerck's research group [Desnerck et al. (2016)].

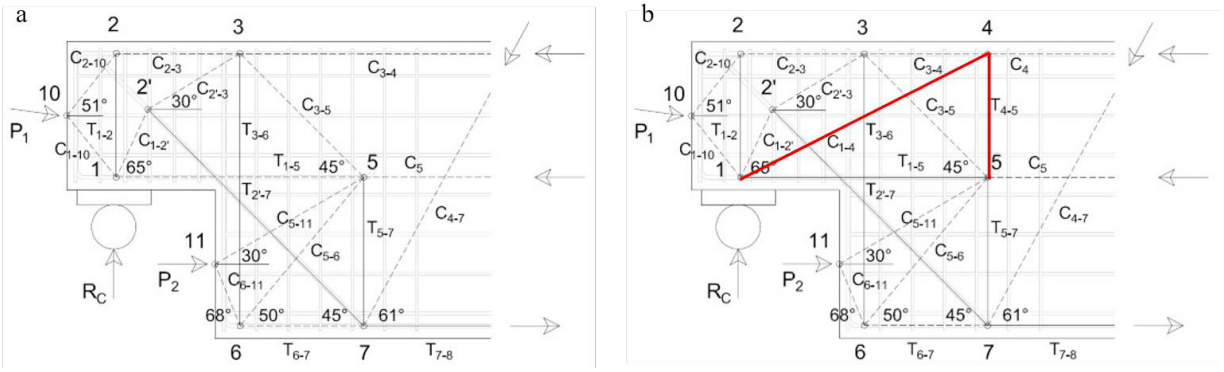

Fig. 4. (a) First stage of the prestressed strut-and-tie model; (b) second stage of the prestressed strut-and-tie model.

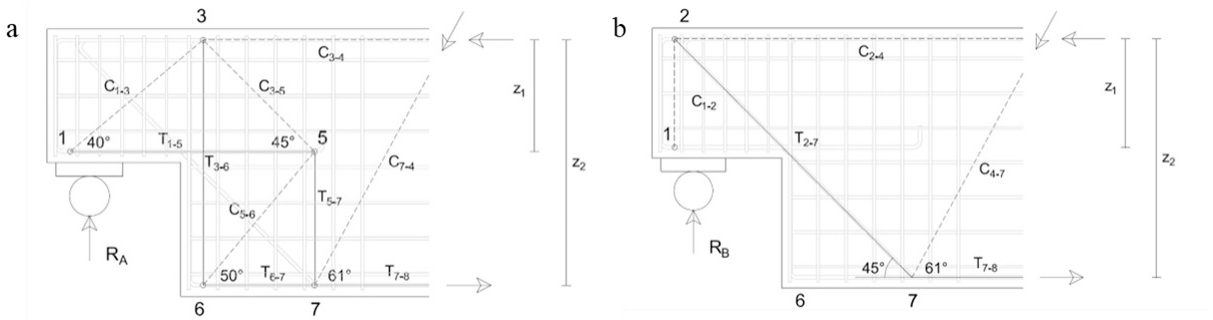

Fig. 5. (a) First strut-and-tie model; (b) second strut-and-tie model.

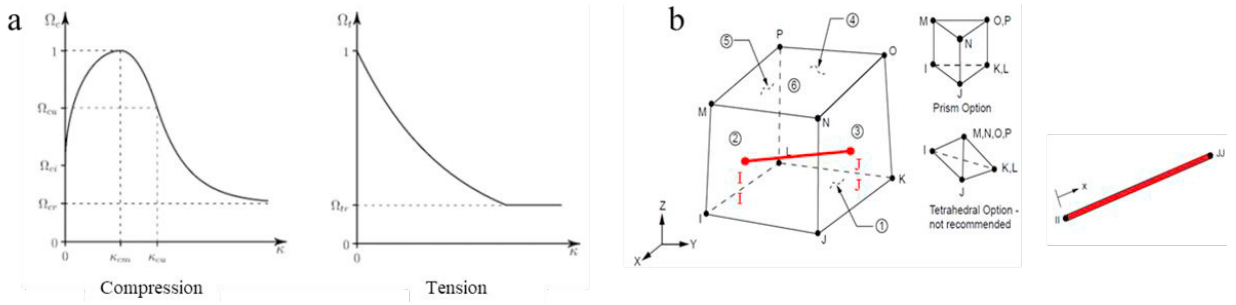

Fig. 6. (a) Menetry-William constitutive law; (b) CPT215 and REIN264 elements.

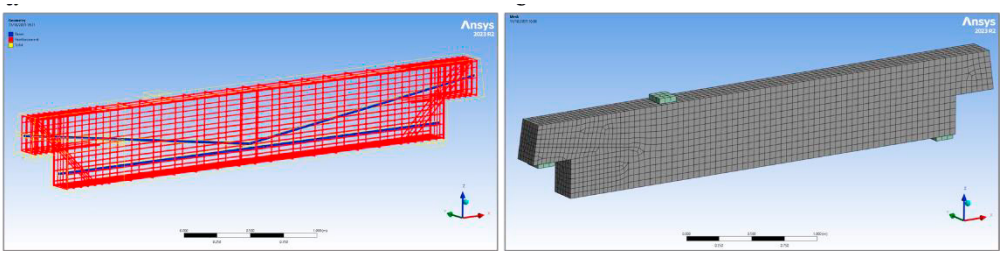

Fig. 7. (a) FE model view; (b) Meshed FE model view.

Nonlinear analyses are performed with admissible large deflections, requiring a minimum of 50 sub-steps and a maximum of 10,000 iterations for the final load to be applied. The analysis of the pre-stressed beams consists of 3 main steps: (*i*) self-weight application, (*ii*) prestressing application, and (*iii*) external load application. For the first two steps, relative slip between prestressing reinforcement and concrete is allowed, while in the last step of analysis, the sliding is prevented by applying a bonded MPC in order to simulate the presence of the grout inside the ducts. The induced corrosion of the half-joint reinforcement for the RL-A1D specimen is included in the model by reducing the cross-sectional area of the rebars subjected to the corrosion phenomena, disregarding effects on the steel ductility promoted by the material degradation. The external load is increasingly applied until the model fails to converge. The results of nonlinear analyses on the specimens are shown in Fig. 8a in terms of capacity curves, reporting the load at the support against the deflection at the load application point.

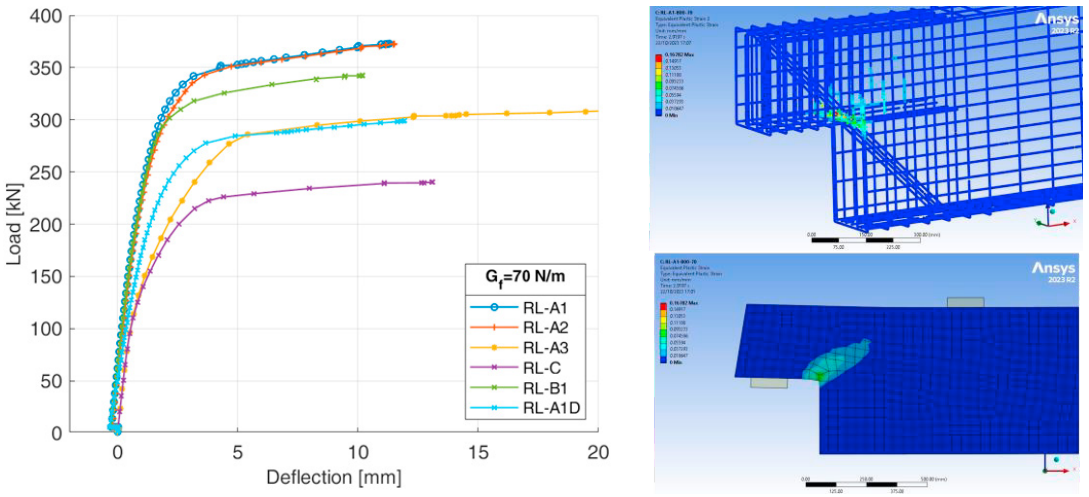

Fig. 8. (a) Capacity curves of the specimens; (b) Equivalent plastic strain on concrete (top) and steel (bottom).

It can be observed that the presence of prestress affects both the shear capacity and the ductility of the resisting mechanism. In detail, the maximum ultimate capacity of 372 kN is obtained with the prestressed specimens RL-A1 and RL-A2, despite the different pre-stress levels. On the contrary, a total absence of prestressing leads to a 16% reduction in ultimate capacity (313 kN) for the same reinforcement layout (RL-A3). As expected, a reduction in the amount of reinforcement (RL-B1) and the absence of prestressing bars (RL-C) leads to a reduction in ultimate capacity of 8 % and 35 %, respectively. Finally, the effects of corrosion on the main reinforcement of the half-joints (RL-A1D) cause a reduction of the overall half-joint capacity of 19%, compared to the expected ultimate capacity of the uncorroded specimen (RL-A1).

For all the specimens, the analyses show the formation of a failure mechanism involving a 45° crack pattern starting from the re-entrant corner of the nib and propagating toward the load point, as the accumulation of plastic deformation on concrete reveals (Fig. 8b top). In the final load steps, the diagonal, horizontal, and vertical main rebars along the concrete cracking zone are extensively hardened, since reinforcements tend to limit the crack opening by accumulating plastic deformation (Fig. 8b bottom).

4. Conclusion

The design of an experimental campaign for investigating the shear behaviour of half-joints of prestressed beams has been presented focusing on the role of tendons with different prestress on the half-joints capacity. At this stage, the influence of tensioned tendons is only addressed numerically, on the basis of the analyses performed to design the tests, by comparing results with those obtained from specimens with non-tensioned tendons and without tendons. In addition, the role of corrosion of the main reinforcement is considered by reducing the reinforcement area.

From a numerical point of view, the studies show, as expected, that the failure mechanism involves the opening and propagation of a crack starting from the re-entrant corner of the nibs. At the ultimate load stages, the yielding and hardening of the vertical and horizontal reinforcements positioned along the cracks are observed. An accurate analysis of the predicted ultimate capacity of the various specimens shows that:

- a reduction of 16% of the prestressing level (640 – 760 MPa) does not affect the ultimate capacity, while the complete loss of prestressing leads to a 16% reduction of the ultimate capacity, compared to the maximum value obtained for specimens with prestressed rebars;
- localized damage due to corrosion on the half-joint reinforcement, in terms of reduction of the reinforcement cross-section area, causes a greater decrease in capacity (19.6%) than reduction of stirrups (RL-B1);
- Strut&Tie models underestimate the capacity obtained from FE analyses.

References

Linee Guida Ponti 2020. Linee guida per la classificazione e gestione del rischio, la valutazione della sicurezza ed il monitoraggio dei ponti esistenti. MIMS, 17 Aprile 2020, Roma.

A. H. Mattock and T. C. Chan, ‘Design and Behavior of Dapped-End Beams’, PCI J., vol. 24, no. 6, pp. 28–45, Nov. 1979, doi: 10.15554/pcij.11011979.28.45

J. Schlaich, K. Schafer, and M. Jennewein, ‘Toward a Consistent Design of Structural Concrete’, PCI J., vol. 32, no. 3, pp. 74–150, May 1987, doi: 10.15554/pcij.05011987.74.150.

D. J. Mader, ‘Detailing Dapped Ends of Pretensioned Concrete Beams’, University of Texas, Austin, 1990.

I.-J. Lin, S.-J. Hwang, W.-Y. Lu, and J.-T. Tsai, ‘Shear strength of reinforced concrete dapped-end beams’, Struct. Eng. Mech., vol. 16, no. 3, Art. no. 3, Sep. 2003.

P. Desnerck, J. M. Lees, and C. T. Morley, ‘Impact of the reinforcement layout on the load capacity of reinforced concrete half-joints’, Eng. Struct., vol. 127, pp. 227–239, Nov. 2016, doi: 10.1016/j.engstruct.2016.08.061.

P. Desnerck, J. M. Lees, and C. T. Morley, ‘The effect of local reinforcing bar reductions and anchorage zone cracking on the load capacity of RC half-joints’, Eng. Struct., vol. 152, pp. 865–877, Dec. 2017, doi: 10.1016/j.engstruct.2017.09.021.

J. Y. Moreno-Martínez and R. Meli, ‘Experimental study on the structural behavior of concrete dapped-end beams’, Eng. Struct., vol. 75, pp. 152–163, Sep. 2014, doi: 10.1016/j.engstruct.2014.05.051.

FABRE, ‘Ispezioni speciali su selle Gerber di ponti esistenti in c.a. e c.a.p. ai sensi delle Linee Guida: la conoscenza e la verifica locale’, Mar. 2022.